Electroweak interactions and the muon $g-2$: Bosonic two-loop effects

T. Gribouk* and A. Czarnecki

Department of Physics, University of Alberta, Edmonton, Alberta, Canada

(Received 4 June 2005; published 30 September 2005)

We present a detailed evaluation of the bosonic two-loop electroweak corrections to the muon's anomalous magnetic moment. We study the Higgs mass dependence and find agreement with a previous evaluation in the large Higgs mass limit. We find $a_\mu^{\mathrm{EW\,bos}}(\text{two-loop}) = (-22.2 \pm 1.6) \times 10^{-11}$, for $114\ \mathrm{GeV} \leq M_{\mathrm{Higgs}} \leq 700\ \mathrm{GeV}$.

DOI: 10.1103/PhysRevD.72.053016 PACS numbers: 12.15.Lk, 14.80.Bn

I. INTRODUCTION

The anomalous magnetic moment of the muon $a_\mu \equiv (g_\mu - 2)/2$ has recently been determined with a very high precision. A series of measurements with positive and negative muons by the E821 Collaboration at the Brookhaven National Laboratory resulted in the present average value [1]

$$a_\mu^{\mathrm{exp}} = (116\,592\,080 \pm 60) \times 10^{-11}. \tag{1}$$

At this level of a one-half part per million precision, this quantity is sensitive to subtle effects predicted by the standard model (SM), including five-loop quantum electrodynamics (QED), hadronic vacuum polarization and light-by-light scattering, and electroweak interactions at two-loops.

Obviously, $g_\mu - 2$ may be affected also by interactions beyond the SM. For this reason, many researchers have analyzed $g_\mu - 2$ in various models of new physics and performed sophisticated studies of the SM effects which are an irreducible background in the search of unknown phenomena. A summary of the SM prediction can be found, for example, in the recent studies and reviews [2–5].

At present, the experimental result in Eq. (1) exceeds the SM prediction by about 2.6 times the combined theoretical and experimental uncertainty. This tantalizing discrepancy may be due to an effect of a new interaction, perhaps supersymmetry. However, it is important to scrutinize the SM prediction before a conclusion can be made. The present paper is devoted to a reevaluation of the largest part of two-loop electroweak diagrams, namely, those without closed fermionic loops.

Electroweak one-loop corrections to $g_\mu - 2$ were among the first quantum effects studied in the renormalizable electroweak theory, in 1972 [6–10]. They were found to increase $g_\mu - 2$ by

$$a_\mu^{\mathrm{EW}}(\text{one-loop}) = \frac{5}{3}\frac{G_\mu m^2}{8\sqrt{2}\pi^2}\left[1 + \frac{(1-4\sin^2\theta_w)^2}{5} + O\left(\frac{m^2}{M^2}\right)\right] \approx 195 \times 10^{-11}, \tag{2}$$

where $G_\mu = 1.16\,639(1) \times 10^{-5}\ \mathrm{GeV}^{-2}$ and weak mixing angle $\sin^2\theta_w = 1 - M_W^2/M_Z^2$. The large mass parameter M represents the mass of a W, Z, or a Higgs boson.

This effect was too small to be measured in the then ongoing CERN experiment. The desire to observe it motivated in part the latest Brookhaven effort.

Two decades after the first electroweak result, Kukhto *et al.* [11] found that an additional virtual photon may significantly modify the one-loop value in Eq. (2). They estimated that effect as a -22% reduction—surprisingly large for hard virtual photons. This and an analogous reduction of the rare muon decay $\mu \to e\gamma$ [12] are due to the large anomalous dimension of the dipole operators such as $\bar{\mu}\sigma^{\mu\nu}\mu F_{\mu\nu}$ and $\bar{e}\sigma^{\mu\nu}\mu F_{\mu\nu}$.

That large effect found in a subset of two-loop electroweak contributions was similar in size to the design precision of the E821 experiment. It therefore appeared as warranted, even necessary, to evaluate the complete two-loop result—a calculation that had not been performed before in the electroweak theory for any other observable.

In 1995 a complete set of 1678 electoweak two-loop diagrams for $g_\mu - 2$ was generated by a computer system [13]. However, such large number of diagrams, many of which are divergent, could not be numerically calculated, at least at that time. Fortunately, it turned out that the majority of those diagrams are strongly suppressed by extra factors of the muon-to-intermediate-boson mass ratio and can be neglected. Thus, a complete two-loop result was found [14]. The numerical value was found to be dominated by large logarithms arising due to photon exchanges and was, somewhat accidentally, close to the value found in its first studies [11,15].

In later work, the renormalization group equation was employed to estimate higher-order logarithmic effects, which however are not sizable [16,17].

The result of [14] was obtained in an approximation assuming that the Higgs boson is sufficiently heavier than the W and Z bosons such that $M_{W,Z}/M_H$ can be

*Electronic address: tgribouk@phys.ualberta.ca

used as an expansion parameter. A recent study [18] relaxed that approximation and found the value of two-loop contributions valid also for a light Higgs (moreover, the two-loop supersymmetric effects were evaluated in that paper).

In this paper, we reanalyze the two-loop electroweak effects. Our goal is to check the previous results and study the Higgs mass dependence. We present our results in a semianalytical form. That is, the dependence on the Higgs mass is presented analytically, while some parts of expressions that depend only on the well-known particle masses are, for the sake of brevity, evaluated numerically. A method employed for obtaining analytical results is also described in some detail.

In this work we focus on diagrams with only bosonic loops (no closed fermion loops). The fermionic subset of corrections was studied separately [19–21]. It was recently the subject of an interesting theoretical controversy which seems to be settled now (see [16] for a thorough discussion and references).

In the next section we briefly explain the asymptotic operation which is the main technical tool used to obtain the analytical result for $g_\mu - 2$. Section III presents partial results for various groups of contributing diagrams. First, we divide all diagrams into five subsets of topologically equivalent diagrams. Then we give analytical or semianalytical results for each topology. Finally we discuss the renormalization procedure and evaluate necessary counterterms, provide the final numerical result, and compare it with the results of Refs. [14,18].

II. TECHNIQUES: ASYMPTOTIC OPERATION AND RESULTING INTEGRALS

The method of asymptotic operation (see [22] for a review and references) has been an invaluable tool in numerous recent studies of effects involving various energy scales. In the present problem, the mass of the muon m sets the soft scale, and the masses of the W, Z, and Higgs bosons—the hard scale: $M_{W,Z,H} \gg m$. As we explained in the introduction, the original study [14] assumed in addition $M_H \gg M_{W,Z}$. Here, we will not assume any hierarchy between $M_{W,Z}$ and M_H at the price of certain complication of our results.

We would like to explain here the basic principles of asymptotic operation. Instead of attempting a rigorous derivation or even a rigorous exposition, we will use a simple example to elucidate the method.

In this study, we are interested in two-loop Feynman graphs G, which have a soft-scale ($\sim m$) external momentum and involve internal lines with both soft-scale and hard-scale ($\sim M$) virtual particles. The exact value of the two-loop integrations is a (possibly very complicated) function of m/M. However, for our purposes it is entirely sufficient to know only an expansion of that function up to m^2/M^2. The purpose of the asymptotic operation is to obtain the desired order of that expansion without having to compute the whole function.

For our purposes, the action of the asymptotic operation on a Feynman graph G may be described with the following formula,

$$\mathrm{As} \circ G = \sum_h (\tau \circ h) \times [G \backslash h]. \tag{3}$$

Let us first of all explain the notation. As $\circ$ G is an expansion of the exact value of G in powers *and logarithms* of m/M. h are the subgraphs of G in which all loop momenta are considered as hard.

Instead of giving an exact definition of which h are relevant, we use as an example the diagram shown in Fig. 1. In that figure, G is shown in picture (a). Subgraphs h are shown in (b)–(e) and range from a single heavy particle line to the whole graph. τ is the Taylor expansion operator, expanding a subgraph in all soft-scale parameters such as the light-particle masses and external momenta of that subgraph (the latter include loop momenta of those loops that are not part of the subgraph). Finally,

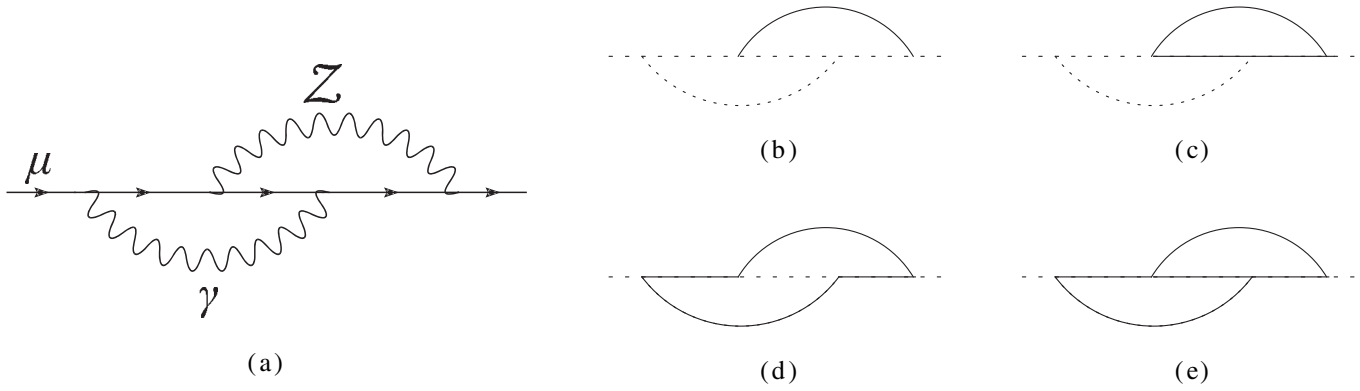

FIG. 1. An example of applying the asymptotic operation to a graph G, shown in (a). (b)–(e) show the full set of subgraphs, as described in the text. Propagators through which hard momenta flow are indicated with solid lines—they constitute a subgraph h. Dashed lines contain only soft-scale momenta and masses—they constitute $G\backslash h$.

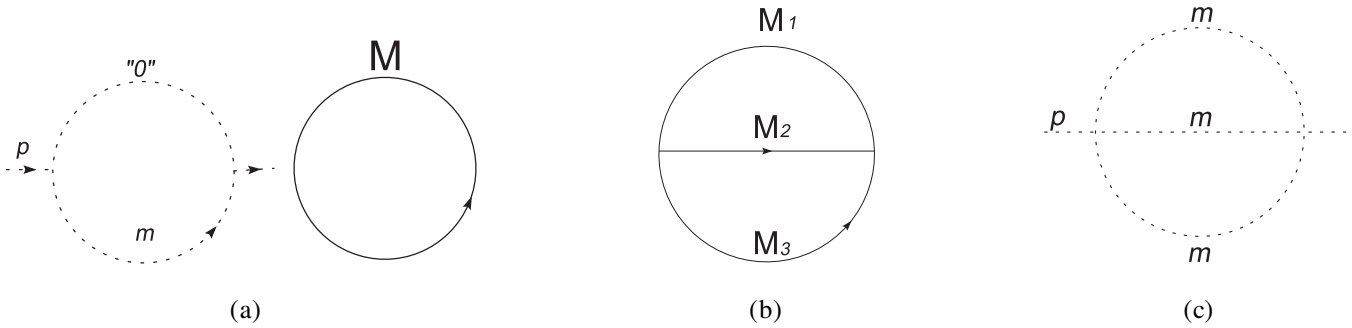

FIG. 2. Basic types of loop integrals needed for the evaluation of two-loop electroweak corrections to $g_\mu - 2$: (a) One-loop light-mass on shell integral multiplied by a one-loop vacuum integral with a large mass; (b) Two-loop vacuum integral (some propagators may be massless ($M = 0$)); (c) Two-loop light-mass on shell integral.

$G\backslash h$ denotes the graph G with the subgraph h contracted into a point. The physical intuition for that concept is such that all masses and loop momenta in $G\backslash h$ are soft; thus, from their point of view, the hard-scale subprocess in h occurs at a very short-distance scale and can be contracted to a point. In other words, the subgraphs h create effective vertices.

What do we gain from this construction? We completely separate soft and hard scales for the purposes of the integration. Thus, the resulting integrals cannot contain both m and M—they factorize into a part that depends only on the soft scales and another that depends on the hard ones. No nontrivial functional dependence on m/M can arise and we obtain the expansion to a given order in m/M by taking a sufficient number of terms in the Taylor expansion of the subgraphs.

The asymptotic operation greatly simplifies the types of integrals that we need to evaluate, as shown in Fig. 2. One-loop on shell integrals and one-loop massive integrals, pictured in Fig. 2(a), are trivial.

Two-loop integrals in Fig. 2(b), dependent on arbitrary masses, were computed in Refs. [23,24]. By means of integration by parts identities [25] the initial integral with arbitrary powers of propagators can be reduced to the integral with all propagators in power one. For the case when all three propagators are massive, we encounter only diagrams with two different masses present. In this simplified case, the general result for such integral, in the dimensional regularization, becomes

$$\begin{aligned} I_{mmM} &\equiv \frac{(4\pi)^d}{\Gamma^2(1+\varepsilon)} \\ &\quad \times \iint \frac{\mathrm{d}^d p \mathrm{d}^d q}{(p^2+m^2)(q^2+m^2)((p+q)^2+M^2)} \\ &= \frac{(m^2)^{1-2\varepsilon}}{(1-\varepsilon)(1-2\varepsilon)}\left[-\frac{1+2z}{\varepsilon^2}+\frac{4z\ln 4z}{\varepsilon}\right. \\ &\quad \left. -2z\ln^2 4z + 2(1-z)\Phi(z)\right], \end{aligned} \tag{4}$$

where $d = 4 - 2\varepsilon$, $z = \frac{M^2}{4m^2}$, and the function Φ is defined as

$$\begin{aligned} \Phi(z) &= 4\left(\frac{z}{1-z}\right)^{1/2}\mathrm{Cl}_2[2\arcsin(z^{1/2})], \\ \mathrm{Cl}_2(\theta) &= -\int_0^\theta d\theta \ln|2\sin(\theta/2)|, \end{aligned} \tag{5}$$

for $z < 1$, and

$$\begin{aligned} \Phi(z) &= \left(\frac{z}{z-1}\right)^{1/2}\left\{-4\mathrm{Li}_2(\xi) + 2\ln^2\xi - \ln^2 4z + \frac{\pi^2}{3}\right\}, \\ \xi &= \frac{1-(\frac{z-1}{z})^{1/2}}{2}, \end{aligned} \tag{6}$$

for $z > 1$.

For the case when one propagator is massless we introduce the function I^{fin}, which is the finite part of the integral $I_{M_c M_a M_b}$ for the case of $M_c = 0$; denoting $R = \frac{M_b^2}{M_a^2}$ we have

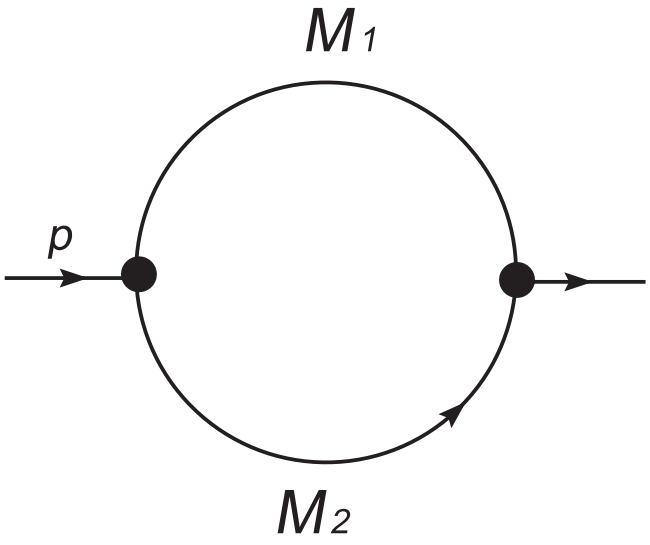

FIG. 3. One-loop massive on shell self-energy integral.

$$I^{\rm fin}(R) = -\frac{7}{2}(1+R) + 3R\ln R - (1-R)\mathrm{Li}_2(1-R) - \frac{R}{2}\ln^2 R. \tag{7}$$

Finally, two-loop on shell integrals shown in Fig. 2(c) can be found, for example, in Ref. [26].

To calculate the renormalization counterterms we shall also need one-loop massive on shell self-energy integrals shown in Fig. 3. They are expressed as linear combinations of integrals of the type (we use $p^2 = -M^2$):

$$S^{ab}(M_1, M_2, M) = \frac{\Gamma(b-2+\varepsilon)}{\Gamma(b)\Gamma(1+\varepsilon)} \int_0^1 \mathrm{d}x \frac{x^a}{[(1-x)(M_1^2 - xM^2) + xM_2^2]^{(b-2+\varepsilon)}}. \tag{8}$$

These integrals can be represented as a series in ε and can be easily computed to the necessary order. We introduce special functions $S^{ab}_{\rm fin}(M_1, M_2, M)$ which represent the finite parts of (8). We shall need only the following cases,

$$\begin{aligned} S^{01}_{\rm fin}(M_1, M_2, M) &= \int_0^1 \mathrm{d}x\{[(1-x)(M_1^2 - xM^2) + xM_2^2][\ln((1-x)(M_1^2 - xM^2) + xM_2^2) - 1]\}, \\ S^{a2}_{\rm fin}(M_1, M_2, M) &= -\int_0^1 \mathrm{d}x x^a \ln[(1-x)(M_1^2 - xM^2) + xM_2^2], \end{aligned} \tag{9}$$

with a taking on the values 0,1 or 2.

III. BOSONIC ELECTROWEAK TWO-LOOP CONTRIBUTIONS IN THE SM

In this section we apply the technique of asymptotic operation, as described in Sec. II, to evaluate all two-loop bosonic contributions. We divide the diagrams into subsets of various topologies and mass assignments and present detailed results for each subset. We display the dependence on the Higgs mass in the analytical form. We also provide details of the renormalization procedure.

Following [14], we use the 't Hooft-Feynman nonlinear gauge [27]. We choose it in such a way that we eliminate the vertex $\gamma W^{\pm} G^{\pm}$. Since $g_\mu - 2$ involves an external photon in every diagram, such choice greatly reduces the number of diagrams. The set of diagrams we have to consider contains all two-loop diagrams one can compose in the SM with the exclusion of pure QED diagrams and diagrams with closed fermion loop; we drop all diagrams with more than one scalar coupling to the muon line, since each such coupling introduces an extra factor $\frac{m_\mu}{M_W}$. Taking advantage of the mirror symmetry we reduce the number of diagrams that must be individually calculated to 138; in addition, some one-loop diagrams must be evaluated for the renormalization.

A. Two-loop topologies and their evaluation

We divide all two-loop diagrams into five topological types, as shown in Fig. 4. Possible insertions of the external photon vertex are indicated with a circle cross, and wavy lines stand for either scalar or vector bosons. Each subset groups diagrams with similar properties with respect to the asymptotic operation and thus can be calculated using the same algebraic code (we use FORM [28] for most algebraic operations). Applying the general formula (3) for the asymptotic operation and computing all resulting integrals, we obtain the following results for the finite parts of various groups of diagrams:

$$\begin{aligned} \mathrm{T1_{A,B,C}} + \mathrm{T2_{A,D,E}} + \mathrm{T3_{A,B,C,D,G}} + \mathrm{T4_{A,D,E,J}} + \mathrm{T5} = &-\frac{\alpha^2}{384\mathrm{c}^2\mathrm{s}^2\pi^2}\{680\mathrm{c}^4 - 362\mathrm{c}^2 - 363 + 6([27 - 30\mathrm{c}^2]\ln m^2 \\ &+ [54\mathrm{c}^2 - 56\mathrm{c}^4]\ln M_W^2 + [56\mathrm{c}^4 - 84\mathrm{c}^2 + 27]\ln M_Z^2)\} \\ &- \alpha^2\frac{m^2}{M_W^2}\left(4.6 - 0.197\ln\frac{m^2}{M_W^2}\right), \end{aligned} \tag{10}$$

$$\begin{aligned} \mathrm{T2_B} = &-\frac{\alpha^2}{576\pi^2}\frac{m^2}{M_W^2}\frac{1}{\Delta^4(\Delta^2-1)}\frac{1}{\mathrm{s}^4}\left\{6\Delta^2\left([2\Delta^6 - 6\Delta^4 + 3\Delta^2 + 1]\Phi\left(\frac{\Delta^2}{4}\right) + [4\Delta^6 - 3\Delta^2 - 4]I^{\rm fin}(\Delta^{-2})\right)\right. \\ &+ \pi^2[3\Delta^4 + \Delta^2 - 4] + 84\Delta^8 + 108\Delta^6 - 111\Delta^4 - 123\Delta^2 - 84 + \ln\Delta^2[96\Delta^6 - 78\Delta^2 - 72] \\ &\left. - 3\ln^2\Delta^2[4\Delta^8 - 8\Delta^6 - 3\Delta^4 + 2\Delta^2 + 8]\right\}, \end{aligned} \tag{11}$$

Topology	M_A	M_B	M_C	M_D	M_E
1_A	M_Z	M_Z	m	m	m
1_B	0	M_Z	m	m	m
1_C	M_Z	M_W	m	0	0

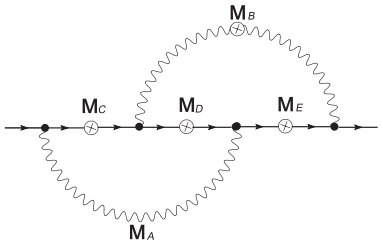

Topology	M_A	M_B	M_C	M_D	M_E
2_A	M_W	M_W	M_Z	0	m
2_B	M_W	M_W	M_H	0	m
2_C	M_Z	M_Z	M_H	0	0
2_D	M_W	M_Z	M_W	0	0
2_E	M_W	M_W	0	0	m
2_F	M_Z	M_H	M_Z	m	m

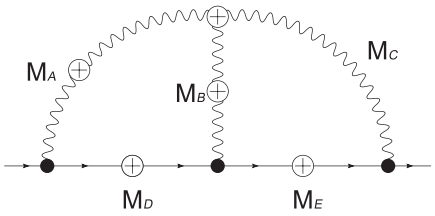

Topology	M_A	M_B	M_C	M_D
3_A	M_W	M_W	M_W	0
3_B	0	0	M_W	m
3_C	M_Z	$M_Z/0$	M_W	m
3_D	M_W	M_W	M_Z	0
3_E	M_W	M_W	M_H	0
3_F	M_Z	M_Z	M_H	m
3_G	M_Z	M_Z	M_Z	m

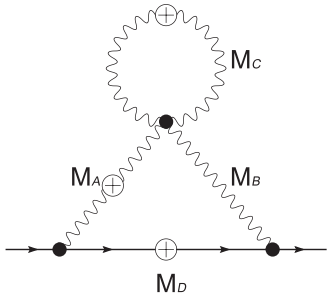

Topology	M_A	M_B	M_C	M_D	M_E
4_A	M_W	M_W	M_Z	M_W	0
4_B	M_W	M_W	M_H	M_W	0
4_C	M_Z	M_Z	M_H	M_Z	m
4_D	M_W	M_W	0	M_W	0
4_E	M_Z	M_Z	M_W	M_W	m
4_F	M_H	0	M_W	M_W	m
4_G	M_H	M_Z	M_W	M_W	m
4_J	0	0	M_W	M_W	m

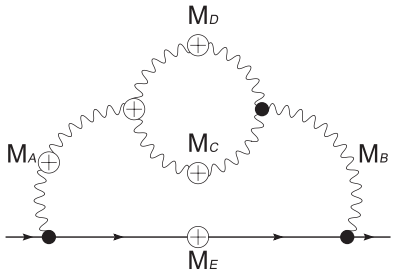

Topology	M_A	M_B	M_C	M_D	M_E
5_A	M_Z	M_Z	m	m	m
5_B	M_W	M_W	0	m	0
5_C	0	M_W	m	0	m
5_D	M_Z	M_W	m	0	m
5_E	M_W	M_Z	0	0	0
5_F	0	M_Z	m	m	m
5_G	M_Z	0	m	m	m

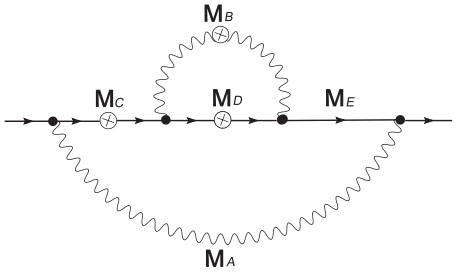

FIG. 4. Diagram topologies and assignments of masses to their lines.

$$\mathrm{T2_C} = -\frac{\alpha^2}{1152\pi^2}\frac{m^2}{M_W^2}\frac{1}{\Lambda^4(\Lambda^2-1)}\frac{(8c^4-12c^2+5)}{c^2s^4}\Big\{3\Lambda^2\Big([\Lambda^6-3\Lambda^4-6\Lambda^2+8]\Phi\Big(\frac{\Lambda^2}{4}\Big) + 2[\Lambda^6-3\Lambda^2-4]I^{\mathrm{fin}}(\Lambda^{-2})\Big) + \pi^2[3\Lambda^4+\Lambda^2-4] + 3[7\Lambda^8+9\Lambda^6-31\Lambda^4-41\Lambda^2-28] + \ln\Lambda^2[24\Lambda^6+18\Lambda^4-78\Lambda^2-72] - 3\ln^2\Lambda^2[\Lambda^8-2\Lambda^6-3\Lambda^4+2\Lambda^2+8]\Big\}, \tag{12}$$

$$\mathrm{T2_F} = \frac{\alpha^2}{192\pi^2}\frac{m^2}{M_W^2}\frac{\Lambda^2}{(\Lambda^2-1)}\frac{(c^2-s^2)}{c^2s^2}\Big\{3[\Lambda^6-7\Lambda^4+14\Lambda^2-8]\Phi\Big(\frac{\Lambda^2}{4}\Big) + 12\Lambda^2[\Lambda^4-4\Lambda^2+1]I^{\mathrm{fin}}(\Lambda^{-2}) + \pi^2\Lambda^2[\Lambda^4-5\Lambda^2+4] + 6[7\Lambda^6-21\Lambda^4-20\Lambda^2+6] + 12\ln\Lambda^2[3\Lambda^4-11\Lambda^2+2] - 3\ln^2\Lambda^2[\Lambda^6-7\Lambda^4+14\Lambda^2-4]\Big\}, \tag{13}$$

$$\mathrm{T3_{E,F}} = -\frac{\alpha^2}{2304\pi^2}\frac{m^2}{M_W^2}\Delta^2\frac{1}{s^4}\{79-336c^2+224c^4+72\ln m^2[1-3c^2+2c^4]+6\ln M_H^2[7-12c^2+8c^4] + 30\ln M_W^2 - 12\ln M_Z^2[5-12c^2+8c^4]\}, \tag{14}$$

$$\mathrm{T4_B} = \frac{\alpha^2}{2304\pi^2}\frac{m^2}{M_W^2}\frac{1}{(\Delta^2-1)}\frac{1}{s^4}\Big\{-18[\Delta^8-6\Delta^6+7\Delta^4+4\Delta^2-6]\Phi\Big(\frac{\Delta^2}{4}\Big) - 36\Delta^4[\Delta^4-3\Delta^2-2]I^{\mathrm{fin}}(\Delta^{-2}) - 126\Delta^8+216\Delta^6+635\Delta^4+650\Delta^2-367-12\Delta^2\ln\Delta^2[12\Delta^4-34\Delta^2-17] + 18\ln^2\Delta^2[\Delta^8-5\Delta^6+4\Delta^4+4\Delta^2] + 60\ln M_W^2[\Delta^4-4\Delta^2+3]\}, \tag{15}$$

$$\mathrm{T4_C} = \frac{\alpha^2}{576\pi^2}\frac{m^2}{M_W^2}\frac{1}{(\Lambda^2-1)}\frac{1}{s^4c^2}\{(\Lambda^2-1)(38\Lambda^2-125+c^2(2c^2-3)(25\Lambda^2-91)) + 18\ln m^2(1-3c^2+2c^4)(\Lambda^4-4\Lambda^2+3) + 3\Lambda^2\ln M_H^2(\Lambda^2-4)(1-6c^2+4c^4) - 3\ln M_Z^2[12-20\Lambda^2+5\Lambda^4+(4c^4-6c^2)(3-8\Lambda^2+2\Lambda^4)]\}, \tag{16}$$

$$\mathrm{T4_F} = -\frac{\alpha^2}{16\pi^2}\frac{m^2}{M_H^2}\frac{1}{\Delta^2}\frac{1}{s^2}\Big\{[6-7\Delta^2]\Phi\Big(\frac{\Delta^2}{4}\Big) + \Delta^2(6+\Delta^2)(\ln\Delta^2-2)\Big\}, \tag{17}$$

$$\mathrm{T4_G} = \frac{\alpha^2}{128\pi^2}\frac{m^2}{M_H^2}\frac{\Lambda^2}{(\Lambda^2-1)}\frac{(4c^2-3)}{s^4}\Big\{\Big[14-3\frac{\Delta^2}{\Lambda^2}+2\frac{(1-6c^2)}{\Lambda^2}\Big]\Phi\Big(\frac{\Delta^2}{4}\Big) + \Big(2\Lambda^2+12c^2-\Delta^2-18+\frac{4\Delta^2}{\Lambda^2}\Big)\Phi\Big(\frac{1}{4c^2}\Big) - \ln\Lambda^2\Big(2\Delta^2+12-\frac{\Delta^4}{\Lambda^2}-2\frac{\Delta^2}{\Lambda^2}\Big)\Big\}. \tag{18}$$

In the above expressions we have dropped the divergences (which cancel in the final sum with the counterterms). We also express all masses in units of $\mu = 1$ GeV. The floating point coefficients in (10) were rounded to provide the precision of 10^{-11} of the final result. They were obtained using $M_W = 80.423$ GeV and $M_Z = 91.1876$ GeV. The functions $\Phi(x)$ and $I^{\mathrm{fin}}(x)$ are defined by means of (5)–(7), respectively. We also use the notations $\Delta \equiv \frac{M_H}{M_W}$, $\Lambda \equiv \frac{M_H}{M_Z}$, $c \equiv \frac{M_W}{M_Z}$, and $s \equiv \sqrt{1-c^2}$.

The results for topologies $T1_A$, $T1_B$, $T1_C$, $T2_A$, $T2_D$, $T2_E$, $T3_A$, $T3_B$, $T3_C$, $T3_D$, $T3_G$, $T4_A$, $T4_D$, $T4_E$, $T4_J$, $T5$ were collected into a single formula because the corresponding diagrams do not contain Higgs propagators and thus can be evaluated without any assumptions about M_H.

B. Renormalization counterterms

Conceptually, the renormalization procedure for our calculation is identical to the one we used in Ref. [14]. The only technical difference is that in our calculation we computed one-loop massive self-energy diagrams precisely, rather than in an expansion to the order of $\sin^6\theta_W$. In this section we briefly review our renormalization procedure and list specific expressions for the W and Z self-energies and for other renormalization constants.

The counterterms for the two-loop EW corrections are generated by renormalizing vertices and propagators in one-loop diagrams. In the nonlinear 't Hooft-Feynman gauge there are just three such diagrams: the Schwinger's QED diagram with a photon loop, its analog with the photon replaced by a Z boson, and a diagram with two W bosons.

The result for Schwinger's diagram in dimensional regularization is given by

$$a^{\mathrm{Schw}} = \frac{\alpha}{2\pi}[1 + \varepsilon(4 - \ln m^2)]. \tag{19}$$

For the calculation of the counterterms we also need the contribution of that diagram with one internal muon propagator squared. It is

$$a_2^{\mathrm{Schw}} = \frac{i\alpha}{2\pi m}[1 + \varepsilon(1 - \ln m^2)]. \tag{20}$$

Using (19) and (20), and bearing in mind that since for the calculation of the EW corrections we dropped the two-loop photonic corrections to the Schwinger diagram and thus have to subtract the photonic contributions from muon mass and wave function renormalization constants as well, we find the counterterm to the a_f at the two-loop level,

$$\begin{aligned} a_{\mathrm{CT}}^{\mathrm{Schw}} = {} & a^{\mathrm{Schw}}\left[\frac{1}{2}(\delta Z_\mu^R + \delta Z_\mu^L - 2\delta Z_\mu^\gamma) + \Sigma'^{AA}(0)\right] \\ & - 2ia_2^{\mathrm{Schw}}(\delta m - \delta m^\gamma). \end{aligned} \tag{21}$$

One-loop contribution of the Z-loop diagram is

$$\begin{aligned} a^Z &= \frac{m^2}{M_Z^2}\frac{\alpha}{4\pi}(g_V^2 V + g_A^2 A), \\ V &\equiv \frac{1}{3} + \varepsilon\left(-\ln m^2 + \frac{2}{3}\ln M_Z^2 - \frac{11}{9}\right), \\ A &\equiv -\frac{5}{3} + \varepsilon\left(\ln m^2 + \frac{2}{3}\ln M_Z^2 - \frac{11}{9}\right). \end{aligned} \tag{22}$$

The corresponding diagram with one muon propagator squared gives

$$a_2^Z = \frac{im^2}{M_Z^2}\frac{\alpha}{4\pi}(g_V^2 - g_A^2)\left[\frac{1}{2} - \varepsilon\left(\frac{1}{2}\ln m^2 + 1\right)\right]. \tag{23}$$

Combining expressions (22) and (23) we obtain the counterterm generated by the Z-loop diagram,

$$\begin{aligned} a_{\mathrm{CT}}^Z = {} & -2ia_2^Z\delta m + \frac{m^2}{M_Z^2}\frac{\alpha}{4\pi}\left[V g_V^2\left(\frac{\delta Z_\mu^R + \delta Z_\mu^L}{2} - \frac{\delta M_Z^2}{M_Z^2} + 2\frac{\delta g_V}{g_V}\right) + A g_A^2\left(\frac{\delta Z_\mu^R + \delta Z_\mu^L}{2} - \frac{\delta M_Z^2}{M_Z^2} + 2\frac{\delta g_A}{g_A}\right) \right. \\ & \left. + g_V g_A \frac{V + A}{2}(\delta Z_\mu^R - \delta Z_\mu^L) + \frac{2}{3}\varepsilon(g_V^2 + g_A^2)\frac{\delta M_Z^2}{M_Z^2}\right]. \end{aligned} \tag{24}$$

Finally, the one-loop contribution of the diagram with two W bosons is

$$a^W = \frac{m^2}{s^2 M_W^2}\frac{\alpha}{4\pi}\left[\frac{5}{6} + \varepsilon\left(-\frac{5}{6}\ln M_W^2 + \frac{19}{36}\right)\right]. \tag{25}$$

Using this expression we obtain a relatively simple counter term because there is no internal muon line and there are only left-handed couplings,

$$\begin{aligned} a_{\mathrm{CT}}^W = {} & a^W\left(2\delta Z_e - 2\frac{\delta s}{s} + \delta Z_\mu^L - \frac{\delta M_W^2}{M_W^2}\right) \\ & - \frac{5}{6}\frac{m^2}{s^2 M_W^2}\frac{\alpha}{4\pi}\varepsilon\frac{\delta M_W^2}{M_W^2}. \end{aligned} \tag{26}$$

The constants appearing in the expressions (19)–(26) are defined as follows:

$$\begin{aligned} g_V &= \frac{1}{sc}\left(-\frac{1}{2} + 2s^2\right), \qquad g_A = \frac{1}{2sc}, \\ \delta g_A &= -\frac{1}{2sc}\left[\delta Z_e + \left(\frac{s^2}{c^2} - 1\right)\frac{\delta s}{s}\right], \\ \delta g_V &= -\delta g_A + 2\frac{s}{c}\left(\delta Z_e + \frac{1}{c^2}\frac{\delta s}{s}\right), \\ \delta s &= -\frac{c^2}{2s}\left(\frac{\delta M_Z^2}{M_Z^2} - \frac{\delta M_W^2}{M_W^2}\right), \qquad \delta Z_e = \frac{\Sigma'^{AA}(0)}{2}, \\ \Sigma'^{AA}(0) &= \frac{\alpha}{4\pi}\left(-\frac{7}{\varepsilon} + 7\ln M_W^2 - \frac{2}{3}\right), \end{aligned} \tag{27}$$

and $\delta m, \delta Z_\mu^{L,R}$ are the muon mass and wave function renormalization defined as

$$\begin{aligned} \delta m &= \delta m^\gamma + \delta m^Z + \delta m^W, \\ \delta m^\gamma &= m\frac{\alpha}{4\pi}\left(-4 - \frac{3}{\varepsilon} + 3\ln m^2\right), \\ \delta m^Z &= \frac{\alpha}{4\pi}\frac{m}{s^2}\left[-\frac{1}{16} + \frac{1}{8\varepsilon} - \frac{\ln M_Z^2}{8} - \frac{1}{12}\frac{m^2}{M_Z^2}\right] \\ &\quad + \frac{\alpha}{4\pi}\frac{m}{c^2}\left[-\frac{21}{16} - \frac{11}{8\varepsilon} + \frac{11\ln M_Z^2}{8} \right. \\ &\quad \left. + \frac{m^2}{M_Z^2}\left(-\frac{17}{12} + 2\ln\frac{M_Z^2}{m^2}\right)\right] \\ &\quad + m\frac{\alpha}{4\pi}\left[\frac{5}{2} + \frac{3}{\varepsilon} - 3\ln M_Z^2 + \frac{m^2}{M_Z^2}\left(\frac{8}{3} - 4\ln\frac{M_Z^2}{m^2}\right)\right], \\ \delta m^W &= \frac{\alpha}{4\pi}\frac{m}{s^2}\left[-\frac{1}{8} + \frac{1}{4\varepsilon} - \frac{\ln M_W^2}{4} + \frac{1}{12}\frac{m^2}{M_W^2}\right], \end{aligned} \tag{28}$$

and

$$\delta Z_\mu^L = \delta Z_\mu^L(\gamma) + \delta Z_\mu^L(Z) + \delta Z_\mu^L(W),$$
$$\delta Z_\mu^L(\gamma) = \delta Z_\mu^R(\gamma) = \frac{\alpha}{4\pi}\left(-4 - \frac{3}{\varepsilon} + 3\ln m^2\right),$$
$$\delta Z_\mu^L(Z) = \frac{\alpha}{4\pi}\frac{1}{16s^2c^2}\left[(2-4s^2)^2\left(\frac{1}{2} - \frac{1}{\varepsilon} + \ln M_Z^2 - \frac{2m^2}{3M_Z^2}\right) - \frac{2m^2}{3M_Z^2}(7 - 5(1-4s^2)^2)\right],$$
$$\delta Z_\mu^L(W) = \frac{\alpha}{4\pi}\frac{1}{s^2}\left[\frac{1}{4} - \frac{1}{2\varepsilon} + \frac{\ln M_W^2}{2} - \frac{m^2}{3M_W^2}\right],$$
$$\delta Z_\mu^R = \delta Z_\mu^R(\gamma) + \delta Z_\mu^R(Z),$$
$$\delta Z_\mu^R(Z) = \frac{\alpha}{4\pi}\frac{1}{16s^2c^2}\left[16s^4\left(\frac{1}{2} - \frac{1}{\varepsilon} + \ln M_Z^2 - \frac{2m^2}{3M_Z^2}\right) - \frac{2m^2}{3M_Z^2}(7 - 5(1-4s^2)^2)\right], \quad (29)$$

and δM_W^2 and δM_Z^2 are mass renormalization constants.

The expressions (21), (24), and (26) provide all counter terms necessary to renormalize two-loop bosonic corrections to a_μ. Taking the sum of the finite parts of these expressions we obtain for the counterterms,

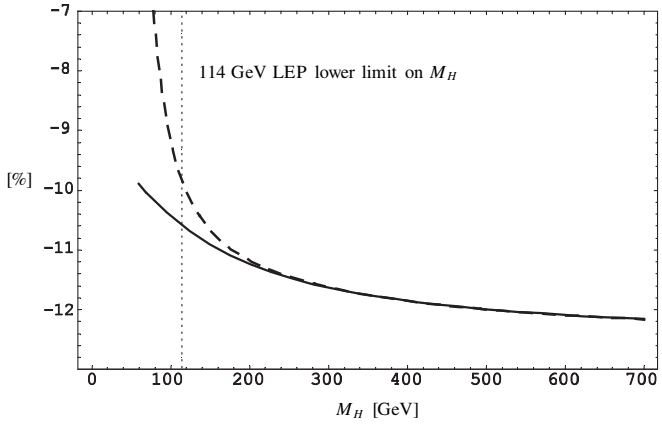

FIG. 5. $\frac{a_\mu^{\rm EW\,(two-loop)}}{a_\mu^{\rm EW\,(one-loop)}}$ as a function of M_H, expressed in percents. Dashed line represents the result from Ref. [14], solid line is the result of this work. The vertical dotted line shows the lower limit for the Higgs boson mass from direct searches, 114 GeV.

$$\begin{aligned}
\mathrm{CT} = {} & \frac{\alpha^2}{384c^2s^2\pi^2}\{680c^4 - 362c^2 - 363 + 6([27-30c^2]\ln m^2 + [54c^2 - 56c^4]\ln M_W^2 + [56c^4 - 84c^2 + 27]\ln M_Z^2)\} \\
& - \alpha^2\frac{m^2}{M_W^2}\left(0.74 + 0.058\ln\frac{m^2}{M_W^2} - 0.111\Delta^2 - 0.0134\Delta^2\ln\Delta^2\right) \\
& - \frac{\alpha^2}{384s^6\pi^2}\frac{m^2}{M_W^2}\left\{\frac{S_{\rm fin}^{01}(M_W, M_W, M_Z)}{M_W^2}(-96 + 475c^2 - 924c^4 + 828c^6 - 256c^8) + (7 - 14c^2 + 4c^4)\right. \\
& \times\left(\frac{S_{\rm fin}^{01}(M_W, M_H, M_W)}{M_W^2} + (1 + 28c^2)\frac{S_{\rm fin}^{01}(M_Z, M_W, M_W)}{M_W^2} + 3S_{\rm fin}^{02}(M_W, M_H, M_W) - (\Delta^2 - 2)S_{\rm fin}^{12}(M_W, M_H, M_W)\right. \\
& \left.\left. - S_{\rm fin}^{22}(M_W, M_H, M_W) - (1 + 48c^2)S_{\rm fin}^{22}(M_Z, M_W, M_W)\right) + (5 - 16c^2 + 8c^4)\right. \\
& \times\left(-c^2\frac{S_{\rm fin}^{01}(M_Z, M_H, M_Z)}{M_W^2} + (1 - 4c^2 + 12c^4)(S_{\rm fin}^{22}(M_W, M_W, M_Z) - S_{\rm fin}^{12}(M_W M_W M_Z)) - 3S_{\rm fin}^{02}(M_Z, M_H, M_Z)\right. \\
& \left. + (\Lambda^2 - 2)S_{\rm fin}^{12}(M_Z M_H M_Z) + S_{\rm fin}^{22}(M_Z M_H M_Z)\right) + (96 - 515c^2 + 1212c^4 - 1404c^6 + 512c^8)S_{\rm fin}^{02}(M_W, M_W, M_Z) \\
& + (-133 + 82c^2 + 322c^4 - 169c^6 + 21c^8)S_{\rm fin}^{02}(M_Z, M_W, M_W) + (217 - 346c^2 - 42c^4 + 29c^6 + 7c^8) \\
& \left.\times S_{\rm fin}^{12}(M_Z, M_W, M_W)\right\}, \quad (30)
\end{aligned}$$

where, as in expression (10), the floating point coefficients were rounded to provide the precision of 10^{-11} of the result and do not depend on M_W and M_Z chosen within experimentally accepted interval. All special functions $S_{a,b}^{fin}$ are defined in Eq. (8).

C. Two-loop corrections to $g-2$

Our result (not yet in its final form—see the next section) for the two-loop bosonic contribution to $g_\mu - 2$ is obtained by adding up all diagrams, Eqs. (10)–(18), and counterterms (30),

$$\begin{aligned}
a_\mu^{\rm EW\,bos}(\text{two-loop}) = {} & T1_{A,B,C} + T2_{A,D,E} + T3_{A,B,C,D,G} \\
& + T4_{A,D,E,J} + T5 + T2_B + T2_C \\
& + T2_F + T3_{E,F} + T4_B + T4_C + T4_F \\
& + T4_G + \mathrm{CT}. \quad (31)
\end{aligned}$$

Its numerical value, normalized to the one-loop correction given in Eq. (2), is plotted in Fig. 5 with a solid line,

for a range of the Higgs boson mass 50 GeV $\leq M_H \leq$ 700 GeV. Also plotted, with a dashed line, is the approximate result of Ref. [14]. We see that both results coincide well for the Higgs boson heavier than about 200 GeV. The only difference in the large Higgs mass region is due to an additional approximation made in Ref. [14], where the difference of the W and Z masses was treated as a small perturbation (first four terms in an expansion in $\sin^2\theta_W$ were retained there). Above $M_H = 250$ GeV, the relative difference between two results is less than 0.1%, well within the precision of the result in Ref. [14]. However, the results differ strongly in the low Higgs mass region. The result of Ref. [14] is not valid in that region since it was obtained under the assumption $M_{W,Z} \ll M_H$. We see that while the result of Ref. [14] seems to grow strongly for the light M_H, the actual bosonic correction (solid line) remains moderate.

D. Reparametrization in terms of G_μ

Equation (31) gives a finite result for the two-loop correction, expressed in terms of the fine structure constant α, the W mass, and the weak mixing angle. Some of the corrections computed in this way are universal for all weak processes and it is convenient to include them in the lower order result by expressing it in terms of the Fermi constant G_μ. This amounts to the substitution, to be made in all components of Eq. (31),

$$\frac{e^2}{8s^2M_W^2} \to \frac{G_\mu}{\sqrt{2}}(1-\Delta r) \tag{32}$$

with

$$\Delta r = 2\delta Z_e - 2\frac{\delta s}{s} - \frac{\delta M_W^2}{M_W^2} + \frac{\Sigma^W(0)}{M_W^2} + \frac{\alpha}{4\pi s^2}\left(6 + \frac{7-4s^2}{2s^2}\right)\ln c^2. \tag{33}$$

This transformation decreases the central value of the ratio of the two-loop to one-loop corrections by up to 7% (depending on the Higgs mass) and, in addition, reduces its uncertainty, since G_μ has been measured to much better precision than M_W and s.

IV. CONCLUSIONS

We have presented a detailed evaluation of the two-loop bosonic corrections to $g_\mu - 2$. Our result confirms the previous approximate evaluation in the limit of the heavy Higgs boson [14]. Our final number for this correction is

$$a_\mu^{\text{EW bos}}(\text{two-loop}) = (-22.2 \pm 1.6)\times 10^{-11}, \tag{34}$$

where the central value was computed for the Higgs mass of 200 GeV, and the error encompasses the interval 50 GeV $\leq M_H \leq$ 700 GeV. This is in agreement with the numerical results of an exact study in Ref. [18]. In addition to the numerical result we have provided here a number of semianalytic intermediate results. They give insight into details of our calculation, allow future checks, and simplify the evaluation of the correction for any Higgs boson mass.

The uncertainty in Eq. (34) is due to the unknown Higgs mass and is slightly reduced in comparison with previous estimates based on the approximate evalulation. The main variation of the correction occurs in the relatively low Higgs mass range. Thus, when more stringent limits on M_H are obtained, that uncertainty will quickly decrease. The main uncertainty of the electroweak contributions will then be due to electroweak hadronic effects, as discussed in [16].

ACKNOWLEDGMENTS

This research was supported by the Natural Sciences and Engineering Research Council of Canada. T. G. gratefully acknowledges support by the Golden Bell Jar Department of Physics.

[1] G. W. Bennett *et al.*, Phys. Rev. Lett. **92**, 161 802 (2004).
[2] M. Passera, J. Phys. G **31**, R75 (2005).
[3] K. Melnikov and A. Vainshtein, Phys. Rev. D **70**, 113006 (2004).
[4] M. Davier and W. J. Marciano, Annu. Rev. Nucl. Part. Sci. **54**, 115 (2004).
[5] A. Czarnecki, Nucl. Phys. B Proc. Suppl. **144**, 201 (2005).
[6] K. Fujikawa, B. W. Lee, and A. I. Sanda, Phys. Rev. D **6**, 2923 (1972).
[7] R. Jackiw and S. Weinberg, Phys. Rev. D **5**, 2396 (1972).
[8] G. Altarelli, N. Cabibbo, and L. Maiani, Phys. Lett. B **40**, 415 (1972).
[9] I. Bars and M. Yoshimura, Phys. Rev. D **6**, 374 (1972).
[10] W. A. Bardeen, R. Gastmans, and B. E. Lautrup, Nucl. Phys. **B46**, 319 (1972).
[11] T. V. Kukhto, E. A. Kuraev, A. Schiller, and Z. K. Silagadze, Nucl. Phys. **B371**, 567 (1992).
[12] A. Czarnecki and E. Jankowski, Phys. Rev. D **65**, 113004 (2002).
[13] T. Kaneko and N. Nakazawa, hep-ph/9505278.
[14] A. Czarnecki, B. Krause, and W. Marciano, Phys. Rev. Lett. **76**, 3267 (1996).
[15] E. A. Kuraev, T. V. Kukhto, and A. Schiller, Sov. J. Nucl. Phys. **51**, 1031 (1990).
[16] A. Czarnecki, W. J. Marciano, and A. Vainshtein, Phys. Rev. D **67**, 073006 (2003).

[17] G. Degrassi and G. F. Giudice, Phys. Rev. D **58**, 053007 (1998).
[18] S. Heinemeyer, D. Stockinger, and G. Weiglein, Nucl. Phys. **B699**, 103 (2004).
[19] A. Czarnecki, B. Krause, and W. Marciano, Phys. Rev. D **52**, R2619 (1995).
[20] S. Peris, M. Perrottet, and E. de Rafael, Phys. Lett. B **355**, 523 (1995).
[21] M. Knecht, S. Peris, M. Perrottet, and E. de Rafael, J. High Energy Phys. 11 (2002) 003.
[22] F. V. Tkachev, Sov. J. Part. Nuclei **25**, 649 (1994).
[23] A. I. Davydychev and J. B. Tausk, Nucl. Phys. **B397**, 123 (1993).
[24] F. A. Berends and J. B. Tausk, Nucl. Phys. **B421**, 456 (1994).
[25] F. V. Tkachov, Phys. Lett. **100B**, 65 (1981).
[26] J. Fleischer and M. Yu. Kalmykov, Comput. Phys. Commun. **128**, 531 (2000).
[27] K. Fujikawa, Phys. Rev. D **7**, 393 (1973).
[28] J. A. M. Vermaseren, math-ph/0010025.